

Mutations in a novel gene *Dymeclin* (FLJ20071) are responsible for Dyggve–Melchior–Clausen syndrome

Vincent El Ghouzzi^{1,†}, Nathalie Dagoneau^{1,†}, Esther Kinning^{2,†}, Christel Thauvin-Robinet^{1,†}, Wassim Chemaitilly^{1,†}, Catherine Prost-Squarcioni³, Lihadh I. Al-Gazali⁴, Alain Verloes⁵, Martine Le Merrer¹, Arnold Munnich¹, Richard C. Trembath² and Valérie Cormier-Daire^{1,*}

¹Department of Medical Genetics and INSERM U393, Hôpital Necker Enfants Malades, 75015 Paris, France,

²Division of Medical Genetics, Departments of Genetics and Medicine, Adrian Building University of Leicester, Leicester LE1 7RH, UK, ³CNRS UPRES 3410, Faculté de Médecine, Hôpital Avicennes, 93009 Bobigny Cedex, France, ⁴Faculty of Medicine, United Arab Emirates University, PO Box 17666 Al Ain, United Arab Emirates and

⁵Department of Medical Genetics, Hôpital Robert Debré, 75019 Paris, France

Received October 28, 2002; Revised and Accepted November 22, 2002

DDBJ/EMBL/GenBank accession no. BK000950

Dyggve–Melchior–Clausen syndrome (DMC) is a rare autosomal-recessive disorder, the gene for which maps to chromosome 18q21.1. DMC is characterized by the association of a spondylo-epi-metaphyseal dysplasia and mental retardation. Electron microscopic study of cutaneous cells of an affected child showed dilated rough endoplasmic reticulum, enlarged and aberrant vacuoles and numerous vesicles. As the etiology of the disorder is unknown, we have used a positional cloning strategy to identify the DMC gene. We detected seven deleterious mutations within a gene predicted from a human transcript (FLJ20071) in 10 DMC families. The mutations were nonsense mutations (R194X, R204X, L219X, Q483X), splice site or frameshift mutations (K626N+92aa to stop). The DMC gene transcript is widely distributed but appears abundant in chondrocytes and fetal brain. The predicted protein product of the DMC gene yields little insight into its likely function, showing no significant homology to any known protein family. However, the carboxy terminal end comprises a cluster of dileucine motifs, highly conserved across species. We conclude that DMC syndrome is consequent upon loss of function of a gene that we propose to name *Dymeclin*, which may have a role in process of intracellular digestion of proteins.

INTRODUCTION

Osteochondrodysplasias are a heterogeneous group of conditions due to impaired development of cartilage and bone (1,2). Amongst them, the spondylo-epi-metaphyseal dysplasias (SEMDs) represent a subgroup which includes a number of disorders each defined by the combination of vertebral, epiphyseal and metaphyseal anomalies. Various inherited defects have been identified within this group, including dominant mutations in *Collagen type II* in SEMD Strudwick type (MIM 184250), and recessive mutations of various proteins: a growth regulator (*WISP3*) in progressive pseudo-rheumatoid dysplasia (MIM 208230), a transcription initiation factor kinase (*EIF2AK3*) in Wolcott–Rallison syndrome (MIM 226980), perlecan (*PLC*) in Schwartz–Jampel type 1 (MIM 225800), a sulfation protein (*PAPSS2*) in SEMD Pakistani type (MIM 603005) and a regulator of

chromatin (*SMARCAL1*) in Schimke immuno-osseous dysplasia (MIM 242900) (3–8).

Dyggve–Melchior–Clausen syndrome (DMC, MIM 223800) is an autosomal-recessive disorder characterized by the association of a spondylo-epi-metaphyseal dysplasia and mental retardation (9). The main features are short trunk dwarfism (<–4 SD), microcephaly and psychomotor retardation (10,11) with specific radiological appearances most likely reflecting abnormalities of the growth plates including platyspondyly (flattened vertebral bodies) with notched end plates, metaphyseal irregularities, laterally displaced capital femoral epiphyses, and small iliac wings with lacy iliac crests (12). DMC is progressive and clinical features are reminiscent of a storage disorder, in particular Morquio’s disease (MPS IV, MIM 253010) (13), but the absence of corneal clouding, deafness, valvular disease or mucopolysacchariduria in DMC serves to differentiate the two conditions.

*To whom correspondence should be addressed. Tel: +33 144495163; Fax: +33 144495150; Email: cormier@necker.fr

†The authors wish it to be known that, in their opinion, the first five authors should be considered joint First Authors.

We have recently reported the mapping of the disease gene to a short interval (1.8 cM) on chromosome 18q21.1 ($Z_{\max} = 9.65$ at $\theta = 0$ at locus D18S1126) (14). Interestingly, a locus for Smith–McCort dysplasia (SMC, a similar SEMD to DMC but without mental retardation, MIM 223800) has simultaneously been reported on chromosome 18q12 ($Z_{\max} = 3.04$ at locus D18S450), suggesting that the two disorders may prove to be allelic (15). Taken together, these reports define a 1.8 cM interval encompassing the DMC/SMC locus, defined by a dinucleotide repeat within the transcript *KIAA0427* and the marker D18S363. Here, we now describe seven distinct but deleterious null mutations in a gene encoding a novel protein in a cohort of patients with DMC.

RESULTS

Analysis of positional candidate genes and linkage refinement

Eight known genes and one predicted transcript were identified within the DMC critical region using publicly available sequences. Of these, four were regarded as possible candidate genes based upon known function, namely myosin Vb (MYO5B) which belongs to the class V myosin family that acts as motor for actin-dependent organelle trafficking (16), 3-oxoacyl-CoA thiolase (ACAA2) which encodes a mitochondrial enzyme catalyzing the final step of the mitochondrial fatty acid beta-oxidation (17), MAP-Kinase 4 (MAPK 4) and mothers-against-decapentaplegic-homolog 7 (MADH 7), both required for intracellular signaling. No deleterious sequence variants were identified by direct sequencing of coding regions of any of these genes nor in the four positional candidate genes, RPL17, LIPG, human CpG binding protein gene (hCGBP) and methyl CpG binding domain protein 1 (MBD1) (data not shown).

Of the 10 independently ascertained kindred investigated, seven were known to originate from Morocco. By using additional microsatellite markers, a common disease haplotype was identified in four of these families (families 3–6). Through the identification of presumed ancestral recombination events in these chromosomes, we inferred that the DMC gene resides in an interval between *KIAA0427* and D18S473 (data not shown). We next identified novel polymorphic simple tandem repeats (STs) within this region, which included an intragenic microsatellite repeat, located within sequence from a predicted human mRNA, FLJ20071. Importantly, this informative repeat was found to be homozygous in all DMC subjects within all consanguineous families studied.

Gene characterization and mutational analysis

Initial sequence analysis of the predicted transcript FLJ20071 indicated a gene composed of nine exons. However, more detailed analysis revealed that the predicted sequence was incomplete (see Methods) and using in-silico database scanning and alignment of predicted cDNAs against genomic sequences, we found six additional exons at the 5' end together with two additional exons at the 3' end. Therefore, the gene appears to be composed of 17 exons, spanning 250 kb of

genomic DNA (Fig. 1A) and codes for a predicted protein of 669 amino acids.

Ten DMC families originating from the Middle East or North Africa were investigated by direct sequencing of the FLJ20071 transcript. We designed primers to amplify coding regions of the predicted gene and to include the exon–intron boundaries. A proband from each family was investigated by direct sequencing (primer sequences included as supplemental information). A total of seven distinct mutations were identified (Table 1). In the multiplex kindreds, each mutation was found to co-segregate with the disease, and was homozygous in affected offspring of consanguineous parents (Fig. 1B). In DMC family 6, the affected individual was found to be a compound heterozygote for FLJ20071 mutant alleles. Four of the seven mutations would predict premature stop codons (R194X, R204X, L219X, Q483X). Two mutations were located at either a splice donor (exon 10) or splice acceptor site (exon 12). Finally, one mutation was a single base-pair deletion in the last exon (1877delA). This frameshift mutation predicted a 49 amino acid extension of the putative DMC protein with the last 93 amino acids being missense (K626N+92aa to stop). An identical mutation was identified in several families from Morocco, each sharing the same haplotype (families 3–6). An identical mutation (1252-1G>A) was identified in the two independently ascertained families, both originating from Lebanon.

DMC transcript analysis

RT-PCR analysis of the RNA transcript in fetal brain, osteoblasts, chondrocytes, osteosarcomas, chondrosarcomas, fibroblasts and lymphocytes detected a single amplification product in each of the tissues tested (Fig. 2A). Northern blot analysis detected two RNA species of 5.6 and 3.1 kb, that appear to be expressed at variable levels in most tissues tested (Fig. 2B).

To further investigate the function of the DMC gene product, we carried out sequence motif and homology searches using available databases (see Methods). Blasts against databases of known proteins failed to detect any significant similarity suggesting the DMC gene product to be novel. The predicted protein contains a large number of leucine or isoleucine residues and a total of 17 repeated dileucine motifs. We also identified three putative transmembrane domains, one myristoyl motif at the N terminal site, one N-glycosylation site (NSSR, +4), two O-glycosylation sites (S40, T45) and various putative sites of phosphorylation (Fig. 3A). Finally, a search for homologous protein sequences in various species showed that the carboxy terminal half (including a cluster of eight dileucine motifs between amino acids 285 and 558) is extremely conserved across species (Fig. 3A and B).

Electron microscopy ultrastructural analysis

Electron microscopy analysis of the skin biopsy of an affected child revealed diffuse anomalies in all cutaneous cell types studied and particularly in fibroblasts, macrophages, mastocytes, keratinocytes, melanocytes and sweat glands. In these cells, numerous and large vacuoles containing either myelinic or osmiophilic bodies were observed (Fig. 4A–D). Moreover, a

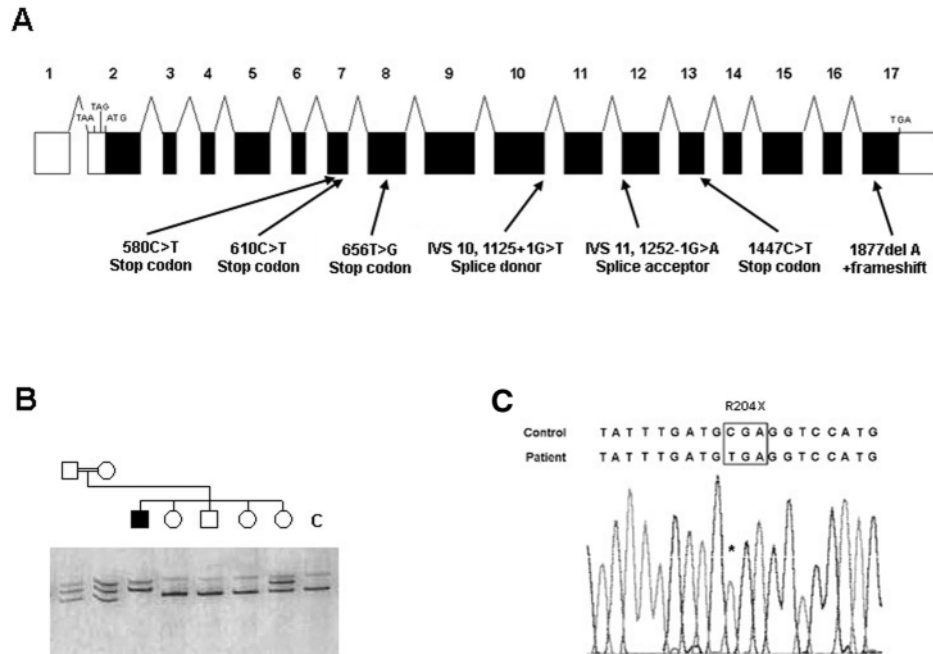


Figure 1. Genomic organization of the DMC gene (*Dymeclin*) with mutations identified in DMC patients. (A) The DMC gene is composed of 17 exons. The ATG initiator and the TGA termination codons are located within exons 2 and 17, respectively. Four different nonsense mutations are shown in exons 7, 8 and 13. Two splice mutations affected the splice donor site of exon 10 (IVS 10) and the splice acceptor site of exon 12 (IVS 11). One frameshift mutation consisting of deletion of an adenine in position 1877 was identified in the last coding exon. (B) SSCP analysis of family 1 showing the segregation of the mutation (R204X) with the disease. (C) Direct sequencing of exon 7 revealed a homozygous C>T transition at position 610, predicted to encode a R204X truncating mutation.

Table 1. *Dymeclin* (FLJ20071) mutations identified in the 10 DMC families

Family number	Ethnic origin	Consanguineous parents	Affected children	Nucleotide change	Amino acid change	Mutated exon	Predicted consequence on the protein
1	Morocco	+	1	610C>T/610C>T	R204X	7	Truncated
2	Morocco	+	2	1447C>T/1447C>T	Q483X	13	Truncated
3	Morocco	+	3	1877delA/1877delA	K626N+frameshift	17	49 amino acid extension
4	Morocco	+	2	1877delA/1877delA	K626N+frameshift	17	49 amino acid extension
5	Morocco	+	1	1877delA/1877delA	K626N+frameshift	17	49 amino acid extension
6	Morocco	-	2	656T>G/1877delA	L219X and K626N+frameshift	8 and 17	50% truncated/ 50% 49 amino acid extension
7	Morocco	+	3	IVS 10 1125+1G>T/ IVS 10 1125+1G>T	—	10 (3'end) splice donor	—
8	Tunisia	+	2	580C>T/580C>T	R194X	7	Truncated
9	Lebanon	-	1	IVS 11 1252-1G>A/ IVS 11 1252-1G>A	—	12 (5'end) splice acceptor	—
10	Lebanon	-	1	IVS 11 1252-1G>A/ IVS 11 1252-1G>A	—	12 (5'end) splice acceptor	—

large number of uncoated vesicles contributing to the enlargement of the vacuoles were observed in fibroblasts (Fig. 4E). Other features included dilated endoplasmic reticulum, and enlarged lysosomes. By contrast, Golgi apparatus and mitochondria were normal.

DISCUSSION

We report nonsense, frameshift and splice mutations in FLJ20071 (a gene identified through bio-informatic sequence analysis) in Dyggve–Melchior–Clausen syndrome, an autosomal

recessive skeletal dysplasia with mental retardation and we propose the name of *Dymeclin* for this novel gene. All but one mutations predicted the generation of a markedly truncated protein. The remaining mutant allele would probably generate an aberrant product, extended at its carboxy terminal end. Hence, this study suggests that loss of function of the DMC gene product is an important mechanism in the pathogenesis of this disease. The same mutations were identified in independently ascertained families on the background of a common haplotype on chromosome 18q21.1 supporting the hypothesis of founder effects within specific ethnic groups.

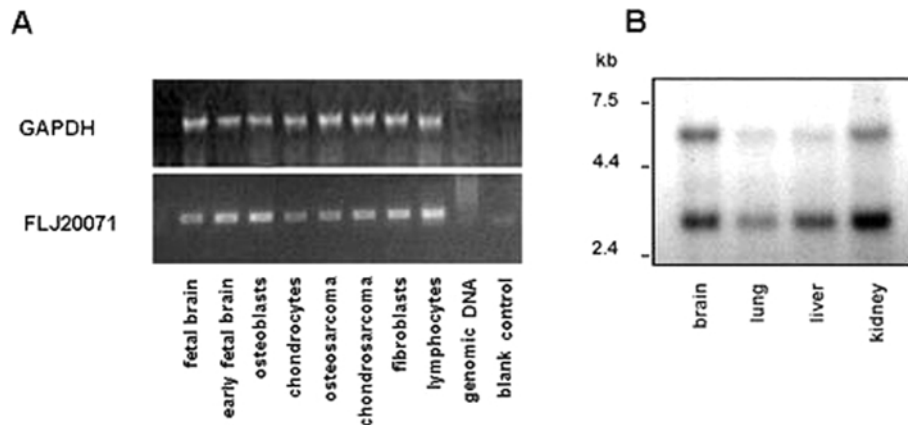


Figure 2. Semi-quantitative RT-PCR and northern blot analyses of the DMC gene (*Dymeclin*) in different human adult, child and fetal tissues. (A) RT-PCR analysis of the DMC gene in three fetal (late fetal brain, 8 weeks fetal brain and chondrocytes), two child (calvarial osteoblasts, and skin fibroblasts) and three adult cell types (chondrosarcoma cells, osteosarcoma cells and lymphocytes) shows that a DMC transcript is detected in all tested cell types. (B) Northern blot analysis of the DMC gene in four human fetal tissues (brain, lung, liver and kidney) reveals the presence of two different transcripts of 3.1 and 5.6 kb.

By reiterative database analysis, we detected eight additional exons and northern blot analysis detected two different transcripts of 3.1 and 5.6 kb in all tissues tested (brain, lung, liver and kidney). Remembering that the clinical manifestations of DMC include skeletal features and mental retardation, it is important to note that the specific transcript was detected in chondrocytes, osteoblasts and brain from the fetal period into adulthood. The disorder is indeed progressive with an increasing severity of manifestations with time.

Based on the clinical features and the progressive nature of the physical signs, DMC has long been considered to arise from the abnormal storage of an unidentified compound. However, metabolic studies have failed to identify an underlying disease mechanism. The function of DMC gene product is yet unknown and the encoded protein does not belong to any known family. However, the high degree of conservation of the carboxy terminal end of the FLJ20071 gene product suggests that this domain plays a key role in the function of the protein. Comparative searches failed to detect any peptide signal but strongly suggested the presence of three transmembrane domains together with a myristoyl site at the amino terminal end. In a number of cases, a myristoylation signal is believed to permit the association of the protein with a membrane (18). Moreover, a large number of dileucine motifs have been identified within the predicted protein and such motifs have been shown to be also involved in trans Golgi sorting, lysosomal targeting and internalization of a number of proteins (19–22).

Our ultrastructural findings in a variety of cutaneous cell types showed normal Golgi and mitochondria but dilated rough endoplasmic reticulum, enlarged and aberrant vacuoles and numerous vesicles. Taken together, these findings suggest that the DMC protein may have a role in digestive cellular processes. Enzymes are required to degrade extracellular material transported into the cells by endocytosis and to digest intracellular structures and macromolecules. Interestingly, biochemical and histochemical analyses in the cartilage and fibrous resting cartilage have shown increased amounts of keratan sulfate with markedly vacuolated chondrocytes and

cytoplasmic inclusions (23–25) and electron microscopy of specimens of growth zone and iliac crest cartilage has also revealed widened cisternae of rough endoplasmic as well as multiple vesicles, suggesting a storage disorder (23).

Based on homology search and electron microscopy study, we conclude that Dyggve–Melchior–Clausen syndrome is due to the loss of function of a protein, encoded by a novel gene, *Dymeclin*, presumably involved in the intracellular digestive process.

MATERIALS AND METHODS

Patients

Ten families were included in the study. Among them, eight have previously been reported including six inbred (families 1, 3–5, 7, 8) and two non-inbred families (families 6 and 9) (14). Two additional families (families 2 and 10) fulfilled the diagnostic criteria for DMC, namely short stature, microcephaly, short trunk with scoliosis and proximal limb shortening and characteristic X-ray manifestations, i.e. double hump, centrally indented vertebral bodies and lacy iliac crest. They were respectively inbred and non-inbred families. Seven families originated from Morocco (1–7), one from Tunisia (8) and two from Lebanon (9,10). All studies had approval of the relevant ethical review committees. The oligonucleotides of the FLJ20071 CA-repeat located in intron 6 were: forward, 5' TCA TCT CTC CCT GCA GTA C 3'; and reverse, 5' CCT GAA TCC ACC AAC ACA G 3'.

Bioinformatics analysis

Computational analysis first predicted the FLJ20071 gene to span 190 kb of genomic DNA with nine exons assigned to locus 18q21.1 on the reverse strand of the chromosome (genomic clone NT_010874, Gi:22058712). Experimental evidence for expression of the putative transcript FLJ20071 was initially assessed by RT-PCR as described below. Blasting several of the predicted exons against human EST databases showed evidence

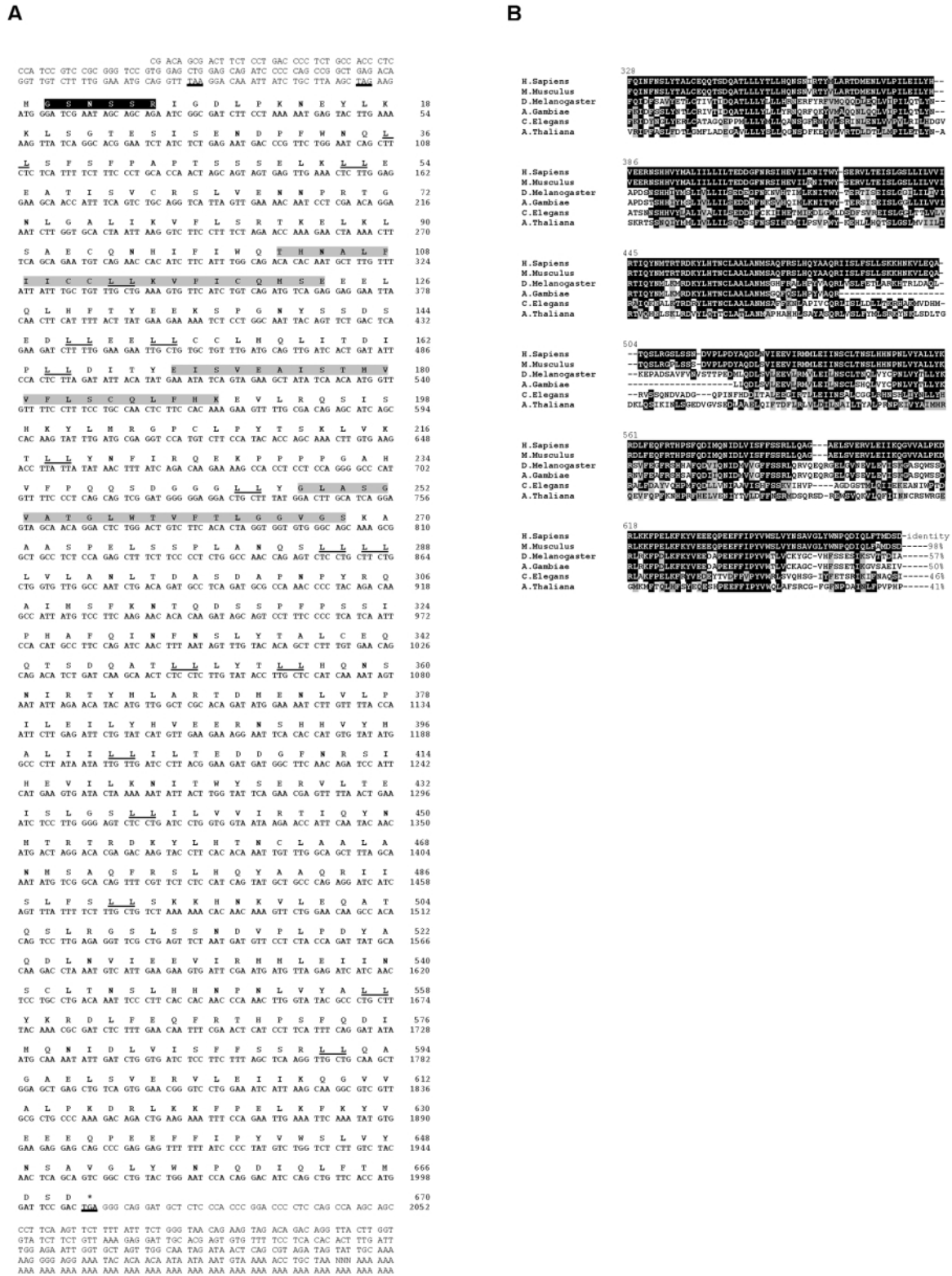


Figure 3. Nucleotide sequence of the compiled cDNA of the human DMC gene (*Dymeclin*), its predicted amino-acid sequence and multiple sequence alignments with other species. (A) Residue 1 is the putative initiator methionine and cDNA nucleotide position +1 is assigned to the first nucleotide of the start codon. The sequence is followed by a poly(A) tail at the 3' end. Three putative transmembrane domains of 21 amino acids are shown in grey and the putative amino-terminal myristoylation site in black. Leucine and isoleucine residues are bold. The dileucine motifs are underlined. (B) Clustal W multiple sequence alignment of the carboxy-terminal half of the DMC gene product showing the high level of sequence conservation between species. Rates of amino acid identity are mentioned. Note that, even between human and plants, the rates of amino acid identity remain strikingly high.

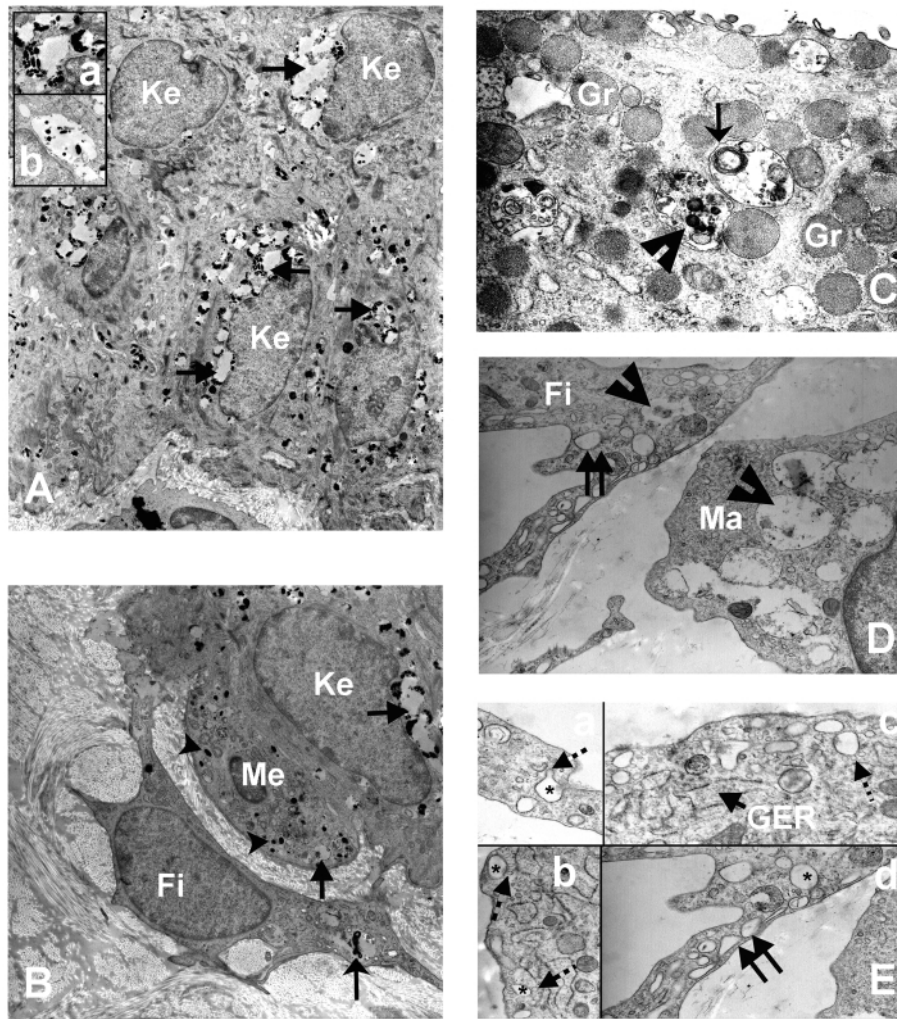


Figure 4. Electron microscopy study of the skin biopsy of a DMC patient. (A) Basal and supra-basal keratinocytes of epidermis. Note the abnormal high number of very large vacuoles (→) which contain melanosomes located either close to the membrane (a) or free in the lumen (b). Ke = keratinocyte. (B) Dermo-epidermal junction showing a basal keratinocyte and a melanocyte in the epidermal layer and a fibroblast in the dermis. Large vacuoles are observed in the three cell types (→), normal melanosomes in the melanocyte cytoplasm (→) and a vacuole containing myelinic bodies in the fibroblast cytoplasm (→). Ke = keratinocyte, Me = melanocyte, Fi = fibroblast. (C) Dark cell of the secretory segment of sweat gland (apical region). The cytoplasm of these cells also display abnormal large vacuoles which contain either myelinic bodies (→) or granular osmiophilic bodies (→) and a large number of phagocytosis vacuoles are also visible along the fibroblast cytoplasmic membrane (→). Fi = fibroblast, Ma = macrophage. (E) Details of the juxta-membrane region in four different fibroblasts. A very large number of uncoated vesicles (a–d, →) are fused together contributing to enlarge the size of vacuoles (*). Note that granular endoplasmic reticulum (GER) looks slightly enlarged (c).

that FLJ20071 has additional corresponding expressed sequences including several that were longer than initially predicted (www.ncbi.nlm.nih.gov/blast). Alignment of the ESTs against genomic sequences of chromosome 18 (clone RP11-110H1, Gi:22653599 and NT_010874, Gi:22058712) finally defined a total of 17 exons, the first of which is likely not translated (5'-UTR). The ATG initiator codon, flanked by a Kozak consensus, is found 53 bp downstream of the beginning of exon 2 and a polyA sequence appears on the cDNA sequence 250 bp downstream of TGA termination codon in exon 17.

To detect homologous sequences to FLJ20071 among either human known sequences or other species sequences, both nBlast and pBlast alignments were performed with different

combinations of databases and full or part of FLJ20071 sequence. Multiple sequence alignments of the carboxy terminal half of FLJ20071 from different orthologs were subsequently performed using the CLUSTAL-W program (26).

Screening the predicted protein sequence for known conserved domains, signal peptide or other motifs was performed by using multiple prediction algorithms available on the web (TopPred (<http://bioweb-pasteur.fr>), PRED-TMR2 (<http://o2.biol.uoa.gr/PRED-TMR2>), PSORT II (<http://psort.nibb.ac.jp>), MYR prediction server (<http://mendel.imp.univie.ac.at/myristate>), PROSITE (<http://cubic.bioc.columbia.edu>), NetPhos 2.0 Prediction (<http://www.cbs.dtu.dk>), SMART (<http://smart.embl-heidelberg.de/smart>), MitoProt II (<http://ihg.gsf.de>).

Mutation detection

Blood samples were obtained with the written consent of the patients and non-affected relatives and genomic DNA was extracted from leukocytes according to standard procedures. A series of 32 intronic primers were designed to amplify the 16 coding exons of the DMC gene. Amplification products were purified and sequenced by using the fluorescent dideoxy-terminator method on an automatic sequencer ABI 377. Silver-staining SSCP was performed to follow the segregation of the identified mutation with the disease in families.

RT-PCR analysis

Total RNAs were extracted using the RNeasy Mini Kit (Qiagen GmbH, Hilden), from either human primary cultured cells (dermal fibroblasts, calvarial osteoblasts, fetal chondrocytes and leukocytes) or human tissues (fetal brain stem, chondrosarcoma and osteosarcoma). Fetal brain cDNA was of commercial origin (Clontech Laboratories, Palo Alto, CA, USA). Complementary DNA was synthesized by priming with random hexamers in the presence of MuLV reverse transcriptase using the manufacturer's protocol (GeneAmp RNA PCR Core Kit, Roche GmbH, Mannheim). Thirty-five to 40 PCR cycles were performed at the annealing temperature of 56°C to amplify a 275 bp fragment specific for the DMC gene (sense and antisense primers were chosen within exon 7 and 9, respectively: 5'-AAGAAGTTT-TGCGACAGAGC-3' and 5'-GGCCAGAGGGGAAGAAAG-3'). Sense and antisense primers used for glyceraldehyde-3-phosphate dehydrogenase (GAPDH) amplification were as follows: 5'-CATGTGGGCCATGAGGTCCACCAC-3' and 5'-TGAAGGTCGGAGTCAACGGATTTGGT-3'.

Northern blot analysis

Pre-made northern blot containing 2 µg of poly(A)+RNA per lane from four human fetal tissues (brain, lung, liver and kidney) was used (Clontech Laboratories). A 0.85 kb cDNA fragment corresponding to the 5'-end of the DMC transcript was obtained by amplification of calvarial osteoblast cDNA (antisense primer was the same as used in RT-PCR analyses and sense primer was chosen within exon 2: 5'-ATGGGATCGAATAGCAGCAG-3'). This fragment was then purified, labeled by random priming (Amersham Pharmacia Biotech, Buckinghamshire, UK) and hybridized overnight in hybridization buffer at 42°C. The blot was washed three times at 42°C with 2× SSC:0.1% SDS for 15 min and once under more stringent conditions at 65°C with 0.1× SSC:0.1% SDS for 20 min. The blot was then exposed to Kodak X-Omat film with an intensifying screen at -80°C.

Electron microscopy

Following informed consent, a DMC patient underwent a 4 mm punch biopsy including the dermis. The sample was fixed in 2.5% glutaraldehyde, post-fixed in 1% osmium-tetroxide, dehydrated in a graded ethanol series and embedded in epon 812. Semi-thin sections (1 µm) were stained with toluidine blue. Ultra-thin sections were selected, contrasted with uranyl acetate and lead citrate and examined with a Philips EM 300 transmission electron microscope.

ACKNOWLEDGEMENTS

We thank Dr Laurence Colleaux for her help and advice. We also wish to thank Drs André Megarbané, Odile Boute, Aziz Sefiani and Smaïl Hadj-Rabia for their clinical assistance. We acknowledge Jean-Paul Monnet for technical assistance for electron microscopy, Noman Kadhom for the cell cultures and Laura Baumber for help with genotyping. Financial support from the Wellcome Trust (R.C.T.) is gratefully acknowledged.

REFERENCES

- Hall, C. (2002) International nosology and classification of Constitutional disorders of bone (2001). *Am. J. Med. Genet.*, **113**, 65–77.
- Dreyer, S.D., Zhou, G. and Lee, B. (1998) The long and the short of it: developmental genetics of the skeletal dysplasias. *Clin. Genet.*, **54**, 464–473.
- Tiller, G.E., Polumbo, P.A., Weis, M.A., Bogaert, R., Lachman, R.S., Cohn, D.H., Rimoin, D.L. and Eyre, D.R. (1995) Dominant mutations in the type II collagen gene, COL2A1, produce spondyloepimetaphyseal dysplasia, Strudwick type. *Nat. Genet.*, **11**, 87–89.
- Hurvitz, J.R., Suwairi, W.M., Van Hul, W., El-Shanti, H., Superti-Furga, A., Roudier, J., Holderbaum, D., Pauli, R.M., Herd, J.K., Van Hul, E.V. *et al.* (1999) Mutations in the CCN gene family member WISP3 cause progressive pseudorheumatoid dysplasia. *Nat. Genet.*, **23**, 94–98.
- Delepine, M., Nicolino, M., Barrett, T., Golamaully, M., Lathrop, G.M. and Julier, C. (2000) EIF2AK3, encoding translation initiation factor 2-alpha kinase 3, is mutated in patients with Wolcott-Rallison syndrome. *Nat. Genet.*, **25**, 406–409.
- Nicole, S., Davoine, C.S., Topaloglu, H., Cattolico, L., Barral, D., Beighton, P., Hamida, C.B., Hammouda, H., Cruaud, C., White, P.S. *et al.* (2000) Perlecan, the major proteoglycan of basement membranes, is altered in patients with Schwartz-Jampel syndrome (chondrodystrophic myotonia). *Nat. Genet.*, **26**, 480–483.
- Xu, Z.H., Otterness, D.M., Freimuth, R.R., Carlini, E.J., Wood, T.C., Mitchell, S., Moon, E., Kim, U.J., Xu, J.P., Siciliano, M.J. and Weinsilboum, R.M. (2000) Human 3' phosphoadenosine 5'-phosphosulfate synthetase 1 (PAPSS1) and PAPSS2: gene cloning, characterization and chromosomal localization. *Biochem. Biophys. Res. Commun.*, **268**, 437–444.
- Boerkoel, C.F., Takashima, H., John, J., Yan, J., Stankiewicz, P., Rosenbarker, L., Andre, J.L., Bogdanovic, R., Burguet, A., Cockfield, S. *et al.* (2002) Mutant chromatin remodeling protein SMARCAL1 causes Schimke immuno-osseous dysplasia. *Nat. Genet.*, **30**, 215–220.
- Dyggve, H.V., Melchior, J.C. and Clausen, J. (1962) Morquio-Ulrich's disease: an inborn error of metabolism? *Arch. Dis. Child.*, **37**, 525–534.
- Toledo, S.P., Saldanha, P.H., Lamego, C., Mourao, P.A., Dietrich, C.P. and Mattar, E. (1979) Dyggve-Melchior-Clausen syndrome: genetic studies and report of affected sibs. *Am. J. Med. Genet.*, **4**, 255–261.
- Beighton, P. (1990) Dyggve-Melchior-Clausen syndrome. *J. Med. Genet.*, **27**, 512–515.
- Spranger, J., Maroteaux, P. and Der Kaloustian, V.M. (1975) The Dyggve-Melchior-Clausen syndrome. *Radiology*, **114**, 415–421.
- Morquio, L. (1929) Sur une forme de dystrophie osseuse familiale. *Bull. Soc. Pédiatr.*, **27**, 145–152.
- Thauvin-Robinet, C., El Ghouzzi, V., Chemaitilly, W., Dagoneau, N., Boute, O., Viot, G., Megarbane, A., Sefiani, A., Munnich, A., Le Merrer, M. and Cormier-Daire, V. (2002) Homozygosity mapping of a Dyggve-Melchior-Clausen syndrome gene to chromosome 18q21.1. *J. Med. Genet.*, **39**, 714–717.
- Ehteshami, N., Cantor, R.M., King, L.M., Reinker, K., Powell, B.R., Shanske, A., Unger, S., Rimoin, D.L. and Cohn, D.H. (2002) Evidence that Smith-McCort Dysplasia and Dyggve-Melchior-Clausen Dysplasia are allelic disorders that result from mutations in a gene on chromosome 18q12. *Am. J. Hum. Genet.*, **71**, 947–951.
- Lapierre, L.A., Kumar, R., Hales, C.M., Navarre, J., Bhartur, S.G., Burnette, J.O., Provance, D.W., Mercer, J.A., Bähler, M. and Goldenring, J.R. (2001) Myosin Vb is associated with plasma membrane recycling systems. *Mol. Biol. Cell*, **12**, 1843–1857.

17. Abe, H., Ohtake, A., Yamamoto, S., Satoh, Y., Amaya Y., Takiguchi, M., Sakuraba, H., Suzuki, Y., Mori, M. and Nimi, H. (1993) Cloning and sequence analysis of a full length cDNA encoding human mitochondrial 3-oxoacyl-CoA thiolase. *Biochem. Biophys. Acta*, **1216**, 304–306.
18. Boutin, J.A. (1997) Myristoylation. *Cell Signal*, **1**, 15–35.
19. Tikkanen, R., Obermuller, S., Denzer, K., Pungitore, R., Geuze, H.J., Von Figura, K. and Honing, S. (2000) The dileucine motif within the tail of MPR46 is required for sorting of the receptor in endosomes. *Traffic*, **1**, 631–640.
20. Sharma, N., Crane, A., Clement, J.P., Gonzalez, G., Babenko, A.P., Bryan, J. and Aguilar-Bryan, L. (1999) The C terminus of SUR1 is required for trafficking of KATP channels. *J. Biol. Chem.*, **274**, 20628–20632.
21. Haft, C.R., Klausner, R.D. and Taylor, S.I. (1994) Involvement of dileucine motifs in the internalization and degradation of the insulin receptor. *J. Biol. Chem.*, **269**, 26286–26294.
22. Ioannou, Y.A. (2000) The structure and function of the Niemann-Pick C1 protein. *Mol. Genet. Metab.*, **71**, 175–181.
23. Engfeldt, B., Bui, T.H., Eklof, O., Hjerpe, A., Reinholt, F.P., Ritzén, E.M. and Wikström, B., (1983) Dyggve-Melchior-Clausen dysplasia. Morphological and biochemical findings in cartilage growth plate. *Acta Paediatr. Scand.*, **72**, 269–274.
24. Horton, W.A. and Scott, C.I. (1982) Dyggve-Melchior-Clausen syndrome: a histo-chemical study of the growth plate. *J. Bone Joint Surg. Am.*, **64**, 408–415.
25. Beck, M., Lucke, R. and Kresse, H. (1983) Dyggve-Melchior-Clausen syndrome: normal degradation of proteodermatan sulfate, proteokeratan sulfate and heparan sulfate. *Clin. Chim. Acta*, **141**, 7–15.
26. Thompson, J.D., Higgins, D.G. and Gibson, T.J. (1994) CLUSTAL W: improving the sensitivity of progressive multiple sequence alignment through sequence weighting, position-specific gap penalties and weight matrix choice. *Nucl. Acids Res.*, **21**, 4673–4680.